

# Square-lattice hybrid organic–inorganic conducting layers in the $\tau$ phase of a TTF tertiary amide derivative†

Pascal Cauliez,<sup>a</sup> Cécile Mézière,<sup>b</sup> Pascale Auban-Senzier,<sup>c</sup> Rodolphe Clérac<sup>d</sup> and Marc Fourmigué<sup>\*a</sup>

Received (in Montpellier, France) 28th January 2008, Accepted 13th March 2008

First published as an Advance Article on the web 8th May 2008

DOI: 10.1039/b801464g

Electrocrystallisation of a TTF tertiary amide derivative, that is EDT-TTF-CONMe<sub>2</sub>, affords a stoichiometric 1 : 1 salt with AuBr<sub>2</sub><sup>−</sup>,  $\tau$ -(EDT-TTF-CONMe<sub>2</sub>)(AuBr<sub>2</sub>)-(TCE)<sub>0.5</sub>, characterised by a hybrid organic–inorganic layer, with AuBr<sub>2</sub><sup>−</sup> anions interspersed between perpendicular cation radicals. This original structure avoids the strong dimerisation gap usually observed in 1 : 1 salts and allows for a strong two-dimensional band dispersion and the absence of gap. The semi conducting behaviour with a high  $\sigma_{RT}$  value (0.025 S cm<sup>−1</sup>) indicates a Mott–Hubbard behaviour.

## Introduction

While most molecular conductors are derived from tetrathiafulvalene derivatives such as TTF, TMTTF or BEDT-TTF with *D*<sub>2h</sub> symmetry,<sup>1</sup> other donor molecules with lower symmetry have been also extensively investigated,<sup>2</sup> either with *C*<sub>2v</sub> symmetry as in EDT-TTF itself or EDT-TTFBr<sub>2</sub>, but also and more recently in fully asymmetric donor molecules such as EDT-TTF-I or EDT-TTF-CONRR'.<sup>3</sup> The latter primary<sup>4</sup> and secondary<sup>5</sup> amides were essentially investigated for the N–H group hydrogen bond donor ability, which was shown to be strongly enhanced in the cation radical salts.<sup>6</sup> On the other hand, the tertiary amide EDT-TTF-CONMe<sub>2</sub> (**1**), which lacks this hydrogen bonding capability, was recently reported to afford a 2 : 1 conducting salt, formulated as (**1**)<sub>2</sub>AsF<sub>6</sub>, which raised a strong interest in the condensed matter community (Chart 1).<sup>7</sup>

Indeed, at variance with the prototypical triclinic mixed-valence (TMTTF)<sub>2</sub>X and (TMTSF)<sub>2</sub>X (X = BF<sub>4</sub><sup>−</sup>, PF<sub>6</sub><sup>−</sup>, ReO<sub>4</sub><sup>−</sup>...) salts where a weak dimerisation of the chains opens a gap at the centre of the 1D band and makes the systems effectively half-filled, in this EDT-TTF-CONMe<sub>2</sub> salt, specific C–H...O=C intra- and inter-stack hydrogen bonds between the ethylenic and carbonyl moieties can favour a regular chain with a strictly 1/4 filled band structure,<sup>8</sup> an issue of paramount importance to determine the relative role of 1/2 and 1/4 filling on the electronic properties of these salts. It is therefore of interest to investigate other salts based on this attractive donor molecule of low symmetry, for example by varying the nature

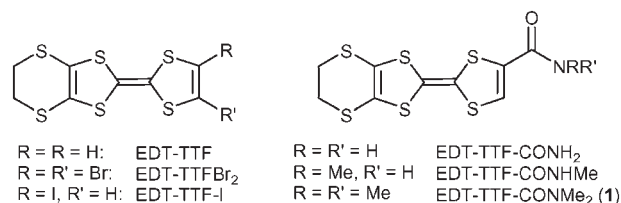


Chart 1 Asymmetrically substituted EDT-TTFs.

of the counter ion in the electrocrystallisation experiments or by substituting some selenium atoms for sulfur atoms in the TTF core. We report here our recent results on the first approach, showing that, in the presence of a linear anion such as AuBr<sub>2</sub><sup>−</sup>, the tertiary amide derivative afforded a novel conducting 1 : 1 phase, as detailed below.

## Results and discussion

Electrocrystallisation of **1**<sup>3</sup> in the presence of <sup>n</sup>Bu<sub>4</sub>NAuBr<sub>2</sub> in 1,1,2-trichloroethane (TCE) afforded after a few days large plate-like crystals on the anode. Note that attempts to obtain a similar phase in the presence of methylene chloride rather than TCE also afforded plate-like crystals which however decomposed very rapidly as they were taken out of the solution, indicating the probable inclusion of CH<sub>2</sub>Cl<sub>2</sub> in these crystals and their rapid desolvation. X-Ray crystal structure resolution showed that the salt obtained in TCE crystallises in the monoclinic system, space group *C*2/*c* (Fig. 1 and Fig. 2), with one donor molecule in a general position in the unit cell and two AuBr<sub>2</sub><sup>−</sup> anions, each located on an inversion centre, together with one TCE molecule, disordered on two positions related by a binary axis. As a consequence, the salt can be described as a 1 : 1 salt [EDT-TTF-CONMe<sub>2</sub>][AuBr<sub>2</sub>](TCE)<sub>0.5</sub>, that is, with each EDT-TTF-CONMe<sub>2</sub> molecule oxidised to the cation radical state corresponding to a full charge transfer ( $\rho = 1$ ). This is further confirmed by the evolution of the intramolecular bond lengths (Table 1) where one observes that the lengthening of the central C=C bond and shortening of the C–S bonds upon oxidation, already noticeable in the 2 : 1 salt of EDT-TTF-CONMe<sub>2</sub> ( $\rho = 0.5$ ),<sup>7</sup> are further enhanced here

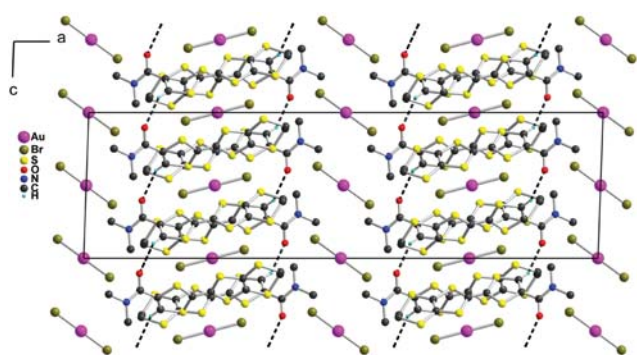
<sup>a</sup> Sciences Chimiques de Rennes, Université Rennes1, UMR CNRS 6226, Equipe MaCSEBât 10C, Campus de Beaulieu, 35042 Rennes, France. E-mail: marc.fourmigue@univ-rennes1.fr

<sup>b</sup> Laboratoire CIMMA, Université d'Angers, UMR CNRS 6200, 2 Bd. Lavoisier, 49045 Angers, France

<sup>c</sup> Laboratoire de Physique des Solides, Université Paris-Sud, UMR CNRS 8502, Bât. 510, 91405 Orsay, France

<sup>d</sup> Université Bordeaux 1, CNRS, Centre de Recherche Paul Pascal (CRPP)- UPR 8641, 115 avenue du Dr A. Schweitzer, 33600 Pessac, France

† CCDC reference number 681961. For crystallographic data in CIF or other electronic format see DOI: 10.1039/b801464g

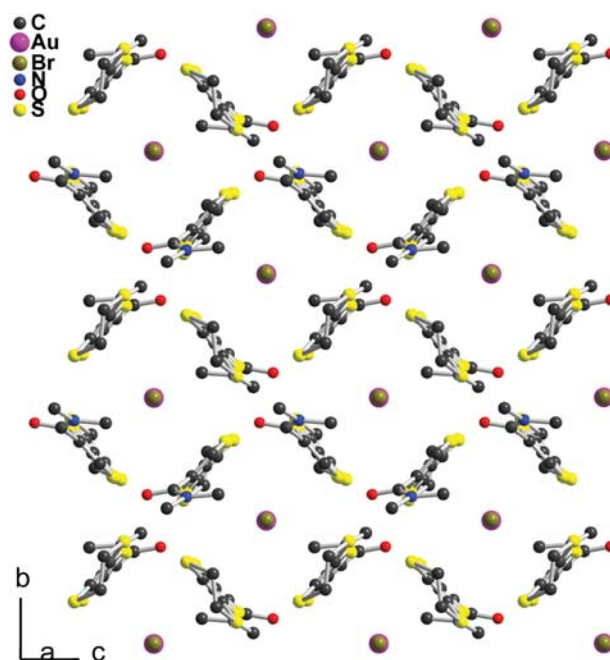


**Fig. 1** Projection view along  $b$  of the unit cell of  $(\mathbf{1})(\text{AuBr}_2) \cdot (\text{TCE})_{0.5}$ . Solvent molecules and all hydrogen atoms (except  $\text{C}_{\text{sp}^2}\text{-H}$  hydrogen atoms) have been omitted for clarity. The black dashed lines indicate the  $\text{C}_{\text{sp}^2}\text{-H} \cdots \text{O}=\text{C}$  hydrogen bond interactions.

in  $(\mathbf{1})(\text{AuBr}_2) \cdot (\text{TCE})_{0.5}$  with  $\rho = 1$ . Note also the angle between the TTF and the  $\text{CONMe}_2$  moieties with a torsion angle for  $\text{C}=\text{C}-\text{C}=\text{O}$  amounts to  $44.5(6)^\circ$  while the molecule was essentially planar in the structures of  $\mathbf{1}$  in its neutral state or its mixed valence  $\text{AsF}_6^-$  salt.

As shown in Fig. 1, the solid state structure of  $(\mathbf{1})(\text{AuBr}_2) \cdot (\text{TCE})_{0.5}$  exhibits a pronounced two-dimensional character, with anionic layers of  $(\text{AuBr}_2^-)_{0.5} \cdot (\text{TCE})_{0.5}$ , alternating along  $a$  with mixed organic-inorganic layers ( $\text{EDT-TTF-CONMe}_2^{+\bullet}(\text{AuBr}_2^-)_{0.5}$ ).

Within the hybrid layers, an intermolecular  $\text{C}_{\text{sp}^2}\text{-H} \cdots \text{O}=\text{C}$  hydrogen bond interaction can be identified with the following structural characteristics ( $\text{C}-\text{H} \cdots \text{O}$ :  $2.62 \text{ \AA}$ ,  $\text{C}(\text{H}) \cdots \text{O}$ :  $3.468(8) \text{ \AA}$  and  $\text{C}-\text{H} \cdots \text{O}$ :  $152.2^\circ$ , which involves the hydrogen atom located *ortho* to the amido group. Note that a similar longer contact was observed in the neutral  $\mathbf{1}$  ( $\rho = 0$ ,  $\text{H} \cdots \text{O}$ :  $2.79 \text{ \AA}$ ) and in  $(\mathbf{1})_2\text{AsF}_6$  ( $\rho = 0.5$ ,  $\text{H} \cdots \text{O}$ :  $2.69 \text{ \AA}$ ). The shortening of this interaction in  $(\mathbf{1})(\text{AuBr}_2) \cdot \text{TCE}$  ( $\rho = 1$ ,  $\text{H} \cdots \text{O}$ :  $2.62 \text{ \AA}$ ) appears to be nicely correlated here with the oxidation degree of the TTF, a recurrent trend identified in various TTF derivatives with hydrogen bonding capabilities<sup>6</sup> and attributed to the activation of the hydrogen bonding donor character of the hydrogen atoms upon TTF oxidation. Very similar  $\text{H} \cdots \text{O}$  distances were also observed in TTF-chloranil where  $\text{C}_{\text{sp}^2}\text{-H} \cdots \text{O}=\text{C}$  interactions play a crucial role in the neutral-to-ionic transition.<sup>9</sup> The layered hybrid structure observed above sharply contrasts with those usually found in cation radical salts of TTF derivatives. Indeed, mixed-valence TTF salts ( $0 < \rho < 1$ ) most often exhibit a strong segregation of the organic and inorganic moieties,




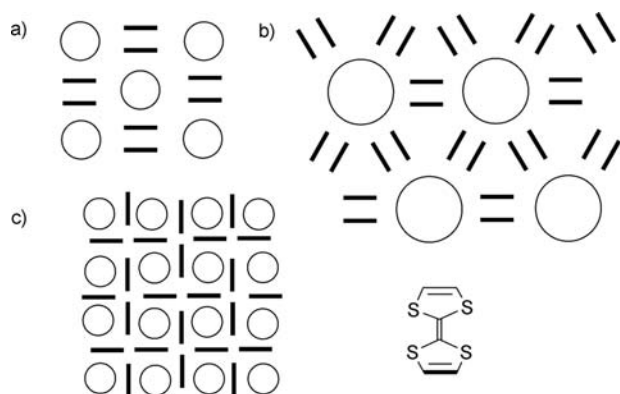
**Fig. 2** Projection view along the  $\text{AuBr}_2^-$  molecular axis, of one hybrid slab in  $(\mathbf{1})(\text{AuBr}_2) \cdot (\text{TCE})_{0.5}$ .

stabilised by the overlap interaction of partially oxidised molecules into 1D or 2D conducting organic structures. On the other hand, fully oxidised TTF salts ( $\rho = 1$ ) recurrently associate into face-to-face  $(\text{TTF})_2^{2+}$  dyads, thus favouring a strong interaction of the two radical species to form bonding and antibonding combinations of the two SOMOs, with the two electrons in the bonding combination. A view of one of the hybrid layers in  $(\mathbf{1})(\text{AuBr}_2) \cdot (\text{TCE})_{0.5}$  (Fig. 2) shows how the organic radical cations and linear  $\text{AuBr}_2^-$  anion are here neatly inter-twinned, with the long axis of the linear  $\text{AuBr}_2^-$  anion essentially parallel to the long axis of the EDT-TTF- $\text{CONMe}_2$  molecule. Each anion is surrounded by four oxidised  $\mathbf{1}^{+\bullet}$  cations while each organic cation exhibits short  $\text{S} \cdots \text{S}$  contacts with five neighbouring molecules. Hence, the slabs are formed of almost perfectly perpendicular TTF molecules held into a square lattice with voids filled by the  $\text{AuBr}_2^-$  anions, without any face-to-face interaction between the oxidised donor molecules.

This unprecedented structural organisation can be compared with other salts obtained with unsymmetrical EDT-TTF derivatives such as  $(\text{EDT-TTF-CN})_2(\text{I}_3)$ <sup>10</sup> or in  $(\text{EDT-TTF-CONH}_2)_6[\text{Re}_6\text{Se}_8(\text{CN})_6]$ ,<sup>11</sup> where hybrid layers are also observed,

**Table 1** Evolution of  $\text{C}=\text{C}$  and  $\text{C}-\text{S}$  (a–d) bond distances (in  $\text{\AA}$ ) in EDT-TTF- $\text{CONMe}_2$  ( $\mathbf{1}$ ) with the charge transfer ( $\rho$ )

						
Compound	$\rho$	C=C	C-S (a)	C-S (b)	C-S (c,d) <sub>av.</sub>	Ref.
Neutral <b>1</b>	0	1.327(10)	1.764(8)	1.756(7)	1.751(7)	3
( <b>1</b> ) <sub>2</sub> (AsF <sub>6</sub> )	0.5	1.364(6)	1.734(4)	1.738(4)	1.730(4)	7
( <b>1</b> )(AuBr <sub>2</sub> )·(TCE) <sub>0.5</sub>	1	1.385(7)	1.719(5)	1.710(5)	1.717(5)	This work

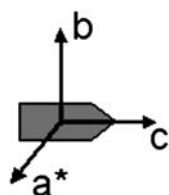


**Scheme 1** Schematic organisation of hybrid layers as found in: (a) (EDT-TTF-CN)<sub>2</sub>(I<sub>3</sub>), (b) (EDT-TTF-CONH<sub>2</sub>)<sub>6</sub>[Re<sub>6</sub>Se<sub>8</sub>(CN)<sub>6</sub>], (c)  $\tau$ -(I)(AuBr<sub>2</sub>)(TCE)<sub>0.5</sub>. The thick lines represent the TTF seen from the side, the white circles represent the anions embedded in the hybrid layers.

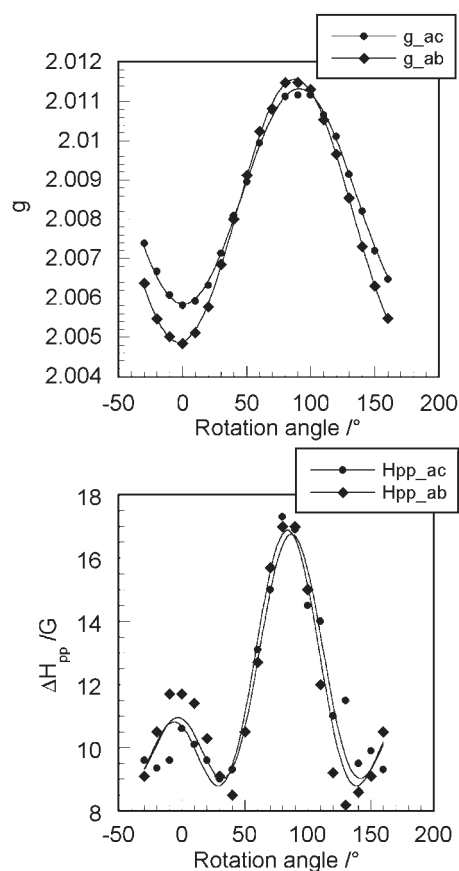
with square symmetry in the former, trigonal symmetry in the latter. In both salts however, as shown in Scheme 1, the EDT-TTF moieties are still associated into dyads, surrounding the inorganic anions. Here in (I)(AuBr<sub>2</sub>)(TCE)<sub>0.5</sub>, the radical molecules do not stabilise into monocationic mixed valence (TTF)<sub>2</sub><sup>•+</sup> or dicationic (TTF)<sub>2</sub><sup>2+</sup> moieties but stay as monomolecular radical cations, a very unusual feature in TTF salts, previously encountered only in the so called  $\tau$  phases. Only a few  $\tau$  phases have been described up to now and systematically with the AuBr<sub>2</sub><sup>−</sup> anion, as for example with the unsymmetrical pyrazino-dimethylethylenedithio-tetrathiafulvalene (P-(S,S)-DMEDT-TTF),<sup>12</sup> or with BEDT-TTF and a mixed tetraiodoethylene-halide inorganic layer.<sup>13</sup> In both examples, non-fractional charge transfer  $\rho$  values were found, with  $\rho \approx 0.875$  in  $\tau$ -(P-(S,S)-DMEDT-TTF)<sub>2</sub>[AuBr<sub>2</sub>]<sub>1</sub>[AuBr<sub>2</sub>]<sub>0.75</sub>,<sup>13</sup> and  $\rho = 1.17$  in  $\tau$ -(BEDT-TTF)<sub>6</sub>(AuBr<sub>2</sub>)<sub>6</sub>Br(TIE)<sub>3</sub>.<sup>14</sup> The salt described here provides thus the first example of a stoichiometric  $\tau$  phase.

The salt possesses a sizeable room temperature conductivity of 0.025 S cm<sup>−1</sup>. Temperature dependence of the conductivity of  $\tau$ -(I)(AuBr<sub>2</sub>)(TCE)<sub>0.5</sub> shows a semiconducting behaviour with an activation energy of 1100–1200 K, that is  $\approx 100$  meV. Electronic paramagnetic resonance (EPR) experiments were performed on an oriented single crystal (Scheme 2), an elongated plate with the largest face index (1 0 0) which confirms the layered nature of the salt with the hybrid layers alternating along  $a$ , as shown in Fig. 1.

No resonance line was observed at room temperature, but on decreasing the temperature one single resonance line appears below 10 K and can be studied at He temperature. Therefore rotation figures were performed at 4 K, first in the ( $a^*$ ,  $c$ ) plane perpendicular to the monoclinic  $b$  axis which is known to be by symmetry a magnetic axis of the system (with the  $c$  direction aligned with the field for a rotation angle of 0°, ● in Fig. 3). As shown in Fig. 3, the  $c$  and  $a^*$  axes appear to be

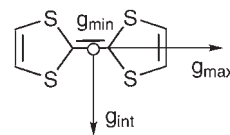


**Scheme 2** Orientation of the single crystal investigated by EPR.

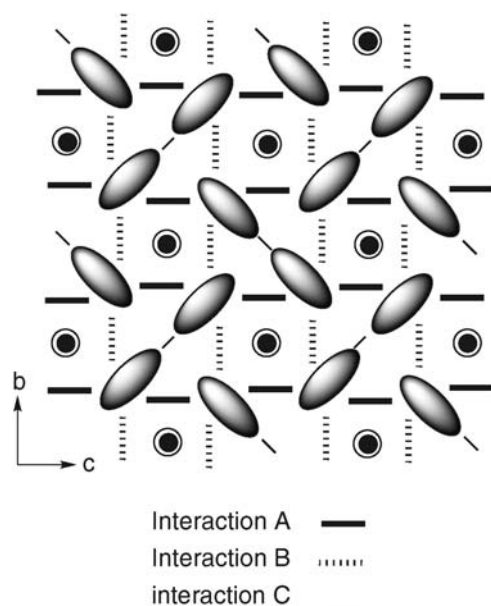


**Fig. 3** Top: rotation pattern of the  $g$  factor with the static magnetic field applied at successive angles from the  $a^*$  direction (at 90° rotation angle) at 4.2 K. Bottom: rotation pattern of the line width ( $\Delta H_{pp}$ ) with the static magnetic field applied at successive angles from the  $a^*$  direction (at 90°) at 4.2 K.

the two other magnetic axes, which is confirmed by the second rotation around the  $c$  axis (with the  $b$  direction aligned with the field for a rotation of 0°, ◆ in Fig. 3). Standard sinusoidal variations are found with extrema of the  $g$  tensor,  $g_{\max} = 2.0114$ ,  $g_{\text{int}} = 2.0058$  and  $g_{\min} = 2.0048$ , essentially aligned along the  $a^*$ ,  $c$  and  $b$  axes, respectively. These values confirm that we are indeed dealing with the intrinsic signal of the TTF cation radicals of this salt and not an impurity line, as one could suspect from its appearance only below 10 K. Indeed, the  $g$  tensor orientation of a TTF cation radical (Scheme 3) is well established,<sup>14</sup> with  $g_{\max}$  along the long axis of the molecule and  $g_{\min}$  perpendicular to the molecular plane. The rotation figures mentioned above demonstrated that the  $g_{\max}$  value was indeed observed along  $a^*$ , that is parallel to the long axis of the TTF molecule while the  $g_{\text{int}}$  and  $g_{\min}$  data obtained here are indeed in the expected range, as also observed in other EDT-TTF amide salts.<sup>7,12</sup>



**Scheme 3** Orientation of the  $g$  tensor of a TTF radical cation.<sup>15</sup>



**Fig. 4** Schematic view of the donor layers showing the three different types of donor...donor intermolecular interactions.

The evolution of the line width with the field orientation is reported in Fig. 3 (bottom). The shape of the rotation figure is characteristic of a low-dimensional spin system and can be satisfactorily fitted here for a two-dimensional system using the following expression:  $\Delta H = A(3\cos^2\alpha - 1)^2 + B$ ,<sup>15</sup> where  $\alpha$  is the angle between the applied magnetic field and the normal to the (*bc*) plane.

In order to understand the origin of the sizeable conductivity of this 1 : 1 salt, we have performed band structure calculations based on tight-binding extended Hückel methods, with preliminary evaluation of the relevant overlap interaction energies ( $\beta_{\text{HOMO-HOMO}}$ )<sup>16</sup> for the different interactions identified in the hybrid planes. As shown in Fig. 4, three different interactions A–C are identified. Interaction A which extends along *c* and interaction B which extends along *b* form an extended two-dimensional square lattice while interaction C links together molecules two by two into inversion-centred dyads. The absolute values of the  $\beta_{\text{HOMO-HOMO}}$  interaction energies as well as the associated S...S intermolecular contacts shorter than 4 Å for the three different interactions are reported in Table 2.

We note that the A and B interactions are fortuitously identical, affording a perfect square lattice network, furthermore interconnected by the inversion centred dyads through the weaker interaction C. All three interactions are surprisingly strong, a primary rationale for the high conductivity (for a 1 : 1 salt). The calculated band structure for a donor layer is reported in Fig. 5. Since there are four different donors per repeat unit within the layer, there are four bands mainly built from the HOMO of 1. As already anticipated from the large and equal  $\beta_A$  and  $\beta_B$  interaction energies, these bands exhibit large and comparable dispersions in the  $\Gamma \rightarrow Y$  and  $\Gamma \rightarrow Z$  directions.

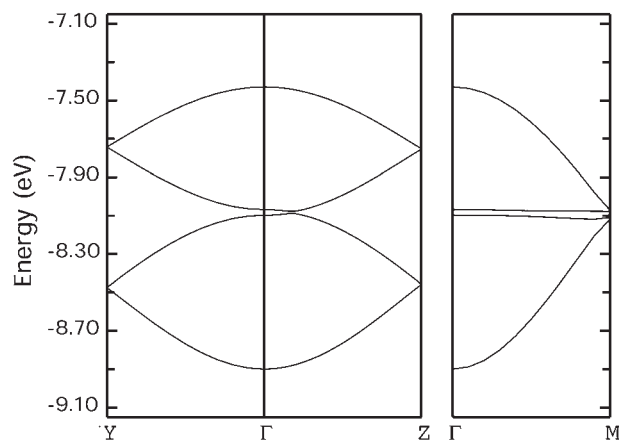
Because of the full charge transfer ( $\rho = 1$ ), the two lower bands are filled while the two upper bands are empty. Calculation of the density of states (DOS) (Fig. 6) shows an absence of

**Table 2** Absolute values of the  $\beta_{\text{HOMO-HOMO}}$  interaction energies with associated S...S intermolecular contacts shorter than 4 Å for the different donor...donor interactions identified in  $\tau$ -(1)(AuBr<sub>2</sub>)(TCE)<sub>0.5</sub>

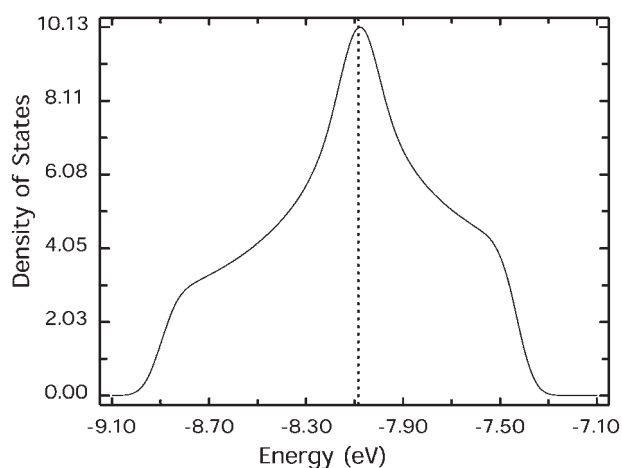
Interaction	S...S distances/Å	$\beta_{\text{HOMO-HOMO}}$ /eV
A	3.480, 3.375, 3.615, 3.538, 3.380	0.302
B	3.362, 3.611, 3.871, 3.618, 3.720	0.302
C	3.512 (×2), 3.930	0.102

gap and thus the possibility of metallic behaviour despite the  $\rho = 1$  charge transfer. This situation has been already encountered in salts of TTM-TTP (TTM-TTP: tetramethylthio-2, 5-bis(1,3-dithiol-3-ylidene)-1,3,4,6-tetrathiapentalene).<sup>17</sup> Therefore the semiconducting character of the salt with this remarkably high conductivity is most probably attributable to a localisation of the charge carriers due to electron–electron correlations, a situation described as a Mott–Hubbard insulator, observed in one-dimensional<sup>18</sup> (TMTTF salts) as well two-dimensional systems such as  $\kappa$ -(BEDT-TTF)<sub>2</sub>Cu[N(CN)<sub>2</sub>]Cl.<sup>19</sup>

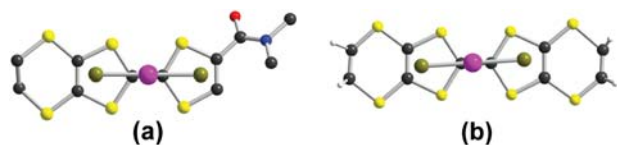
Finally, it should also be stressed that all three known examples of a  $\tau$  phase described so far have been obtained with the linear AuBr<sub>2</sub><sup>−</sup> anion which appears to efficiently stabilise in some way this perpendicular arrangement of the donor molecules, whatever their symmetry, since it was observed with BEDT-TTF itself,<sup>13</sup> with the P-(S,S)-DMEDT-TTF donor molecule with *C*<sub>2</sub> symmetry<sup>12</sup> or here with EDT-TTF-CONMe<sub>2</sub>. The question then arises of a specific stabilising interaction between the TTF cation radical and the AuBr<sub>2</sub><sup>−</sup> anion, an interaction which would be strong enough in some cases to compete with the usual face-to-face stacking of the TTF cation radicals into localised dyads, or extended stacks or slabs. It is also based on the observation (Fig. 7) of an essentially eclipsed overlap between the TTF radical cation and the AuBr<sub>2</sub><sup>−</sup> anion with C...Au distances around 3.75 Å, that is, shorter than the sum of van der Waals radii. Theoretical studies of the interaction between ethylene and metallic gold have been reported earlier<sup>20</sup> but it would now of interest to investigate a more complex system such as



**Fig. 5** Calculated band structure for a donor layer of salt  $\tau$ -(1)(AuBr<sub>2</sub>)(TCE)<sub>0.5</sub>, where  $\Gamma = (0, 0)$ ,  $Y = (b^*/2, 0)$ ,  $Z = (0, c^*/2)$ , and  $M = (b^*/2, c^*/2)$ .



**Fig. 6** Calculated density of states (DOS) for the bands built out of the HOMO of the EDT-TTF-CONMe<sub>2</sub> molecules. The dotted line represents the calculated Fermi level for the  $\rho = 1$  charge transfer.



**Fig. 7** One of the overlap interactions between the TTF cation radical and AuBr<sub>2</sub><sup>−</sup> in: (a)  $\tau$ -(1)(AuBr<sub>2</sub>)<sub>2</sub>·(TCE)<sub>0.5</sub>, (b)  $\tau$ -(BEDT-TTF)<sub>6</sub>(AuBr<sub>2</sub>)<sub>6</sub>Br(TIE)<sub>3</sub>.<sup>13</sup>

the TTF<sup>+</sup>•/AuBr<sub>2</sub><sup>−</sup> pair, based on this assumption of a possible stabilising interaction.

## Conclusion

A rare stoichiometric  $\tau$  phase has been identified in the 1 : 1 salt  $\tau$ -(EDT-TTF-CONMe<sub>2</sub>)<sub>2</sub>(AuBr<sub>2</sub>)<sub>2</sub>·TCE. It is characterised by a square lattice of orthogonal radical cations surrounding one AuBr<sub>2</sub><sup>−</sup> anion, giving rise to mixed conducting layers, separated from each other by AuBr<sub>2</sub><sup>−</sup> anion and solvent molecules. Band structure calculations confirm the square lattice nature of the network with an absence of gap in the density of states. The sizeable conductivity ( $\sigma_{RT} = 0.025 \text{ S cm}^{-1}$ ) of this 1 : 1 salt is attributable to a localisation of the charge carriers due to electron–electron correlations, a situation described as a Mott–Hubbard insulator.

## Experimental

**Electrocrystallisation experiments.** The EDT-TTF-CONMe<sub>2</sub> molecule<sup>3</sup> and the <sup>18</sup>Bu<sub>4</sub>NAuBr<sub>2</sub> salt<sup>21</sup> were prepared as previously described. A two compartment cell equipped with Pt electrodes (diameter 1 mm, length 1.5 cm) with freshly distilled 1,1,2-trichloroethane (TCE) was used with <sup>18</sup>Bu<sub>4</sub>NAuBr<sub>2</sub> (100 mg) and **1** (10 mg). Constant current (1  $\mu$ A) was applied for 14 days, affording plate-like crystals on the anode.

**Crystallography.** The crystal was mounted on the top of a thin glass fiber with Araldite glue. Data were collected on an Enraf-Nonius CCD diffractometer at 293 K with

graphite-monochromated Mo-K $\alpha$  radiation ( $\lambda = 0.71073 \text{ \AA}$ ). The structure was solved by direct methods (SHELXS97) and refined (SHELXL-97)<sup>22</sup> by full-matrix least-squares methods, as implemented in the WinGX software package.<sup>23</sup> Absorption correction was applied. Hydrogen atoms of **1** were introduced at calculated positions (riding model), included in structure factor calculations but not refined.

A 1,1,2-trichloroethane (TCE) molecule was found disordered on a two-fold axis and difficult to model properly, hence an anomalously short C–C bond. As a consequence, the carbon atom of the TCE was refined only isotropically and hydrogen atoms were not introduced on TCE.

Crystal data for (1)<sub>2</sub>(AuBr<sub>2</sub>)<sub>2</sub>·(TCE): C<sub>24</sub>H<sub>25</sub>Au<sub>2</sub>Br<sub>4</sub>Cl<sub>3</sub>·N<sub>2</sub>O<sub>2</sub>S<sub>12</sub>,  $M_r = 1578.15$ ,  $T = 293(2) \text{ K}$ , monoclinic, space group  $C2/c$ ,  $a = 37.1481(5)$ ,  $b = 11.0741(2)$ ,  $c = 10.5643(2) \text{ \AA}$ ,  $\beta = 92.0260(10)^\circ$ ,  $V = 4343.24(13) \text{ \AA}^3$ ,  $\rho_{\text{calc}} = 2.413 \text{ g cm}^{-3}$ ,  $\mu = 11.219 \text{ mm}^{-1}$ ,  $Z = 4$ , refl. collected: 45 469, ind. refl.: 4979 ( $R_{\text{int}} = 0.112$ ), final  $R$  indices [ $I > 2\sigma(I)$ ]:  $R_1 = 0.0423$ ,  $wR_2 = 0.1213$ ,  $R$  indices (all data):  $R_1 = 0.0523$ ,  $wR_2 = 0.1305$ .

**EPR experiments.** EPR experiments were performed on a Bruker ESP-300E X band spectrometer (operating at a microwave frequency of 9.3 GHz) equipped with an ESR900 Oxford cryostat. To realise the experiment, a selected crystal has been oriented on a quartz rod and the EPR line is studied for along the different magnetic orientations of the crystal.

**Band structure calculations.** The tight-binding calculations used an extended-Hückel-type Hamiltonian,<sup>24</sup> as implemented in the Caesar 1.0 chain of programs.<sup>25</sup> The off-diagonal matrix elements of the Hamiltonian were calculated according to the modified Wolfsberg–Helmholz formula.<sup>26</sup> All valence electrons were explicitly taken into account in the calculations, and the basis set consisted of double- $\zeta$  Slater-type orbitals for C, H, O, N and S and single- $\zeta$  Slater-type orbital for H was used. The exponents, contraction coefficients, and atomic parameters were taken from previous work.<sup>27</sup>

## Acknowledgements

This work was supported by the CNRS, The Université Bordeaux 1, The Région Aquitaine and the Agence Nationale de la Recherche (ANR) program no NT05-2 42710.

## References

- 1 See the special *Chem. Rev.* issue on Molecular Conductors, ed. P. Batail, *Chem. Rev.*, 2004, **104** (11).
- 2 J.-M. Fabre, *Chem. Rev.*, 2004, **104**, 5133.
- 3 K. Heuzé, M. Fourmigué and P. Batail, *J. Mater. Chem.*, 1999, **9**, 2373.
- 4 K. Heuzé, M. Fourmigué, P. Batail, E. Canadell and P. Auban-Senzier, *Chem.–Eur. J.*, 1999, **5**, 2971.
- 5 K. Heuzé, C. Mézière, M. Fourmigué, P. Batail, C. Coulon, E. Canadell, P. Auban-Senzier and D. Jérôme, *Chem. Mater.*, 2000, **12**, 1898.
- 6 M. Fourmigué and P. Batail, *Chem. Rev.*, 2004, **104**, 5379.
- 7 K. Heuzé, M. Fourmigué, P. Batail, C. Coulon, R. Clérac, E. Canadell, P. Auban-Senzier, S. Ravy and D. Jérôme, *Adv. Mater.*, 2003, **15**, 1251.
- 8 For other examples see also: (a) J.-M. Fabre, L. Giral, E. Dupart, C. Coulon and P. Delhaes, *J. Chem. Soc., Chem. Commun.*, 1983,

- 426; (b) P. Delhaes, E. Dupart, J. Amiel, C. Coulon, J.-M. Fabre, L. Giral, D. Chasseau and B. Gallois, *J. Phys. Colloq.*, 1983, **44**, 1239.
- 9 P. Batail, S. J. LaPlaca, J. J. Mayerle and J. B. Torrance, *J. Am. Chem. Soc.*, 1981, **103**, 951.
- 10 T. Devic, J. N. Bertran, B. Dornier, E. Canadell, N. Avarvari, P. Auban-Senzier and M. Fourmigué, *New J. Chem.*, 2001, **25**, 1418.
- 11 S. A. Baudron, P. Batail, C. Coulon, R. Clérac, E. Canadell, V. Laukhin, R. Melzi, P. Wzietek, D. Jérôme, P. Auban-Senzier and S. Ravy, *J. Am. Chem. Soc.*, 2005, **127**, 11785.
- 12 J. S. Zambounis, J. Pfeiffer, G. C. Papavassiliou, D. J. Lagouvardos, A. Terzis, C. P. Raptopoulou, P. Delhaes, L. Ducasse, N. A. Fortune and K. Murata, *Solid State Commun.*, 1995, **95**, 211.
- 13 H. M. Yamamoto, J.-I. Yamaura and R. Kato, *J. Am. Chem. Soc.*, 1998, **120**, 5905.
- 14 W. M. Walsh, Jr, L. W. Rupp, Jr, F. Wudl, M. L. Kaplan, D. E. Schafer, G. A. Thomas and R. Gemmer, *Solid State Commun.*, 1980, **33**, 413.
- 15 P. M. Richards and M. B. Salamon, *Phys. Rev. B: Solid State*, 1974, **9**, 32.
- 16 M.-H. Whangbo, J. M. Williams, P. C. W. Leung, M. A. Beno, T. J. Emge and H. H. Wang, *Inorg. Chem.*, 1985, **24**, 3500.
- 17 (a) T. Mori, H. Inokuchi, Y. Misaki, T. Yamabe, H. Mori and S. Tanaka, *Bull. Chem. Soc. Jpn.*, 1994, **67**, 661; (b) T. Mori, *Chem. Rev.*, 2004, **104**, 4947, and references therein.
- 18 D. Jérôme, *Chem. Rev.*, 2004, **104**, 5565.
- 19 M. Dressel and N. Drichko, *Chem. Rev.*, 2004, **104**, 5689.
- 20 G. Nicolas and F. Spiegelmann, *J. Am. Chem. Soc.*, 1990, **112**, 5410.
- 21 P. Braunstein and R. J. H. Clark, *J. Chem. Soc., Dalton Trans.*, 1973, 1845.
- 22 G. M. Sheldrick, SHELX97-Programs for Crystal Structure Analysis (Release 97-2), 1998.
- 23 L. J. Farrugia, *J. Appl. Crystallogr.*, 1999, **32**, 837.
- 24 M.-H. Whangbo and R. Hoffmann, *J. Am. Chem. Soc.*, 1978, **100**, 6093.
- 25 J. Ren, W. Liang and M.-H. Whangbo, *Crystal and Electronic Structure Analysis Using CAESAR*, 1998.
- 26 J. H. Ammeter, H.-B. Bürgi, J. Thibeault and R. Hoffmann, *J. Am. Chem. Soc.*, 1978, **100**, 3686.
- 27 S. A. Baudron, N. Avarvari, E. Canadell, P. Auban-Senzier and P. Batail, *Chem.-Eur. J.*, 2004, **10**, 4498.